*Inflammation, Vol. 42, No. 5, October 2019 (© 2019)*
DOI: 10.1007/s10753-019-01051-9

ORIGINAL ARTICLE

# Diet-Induced Pulmonary Inflammation and Incipient Fibrosis in Mice: a Possible Role of Neutrophilic Inflammation

**M. C. Della Vedova,[1,2] F. M. Soler Garcia,[3] M. D. Muñoz,[1,2] M. W. Fornes,[4] Sandra E. Gomez Mejiba,[1,2,6] N. N. Gómez,[5] and Dario C. Ramirez[1,6]**

*Abstract*— Chicken fat and fructose are added into food-processing to reduce costs and enhance acceptability; however, these additives turn food into unhealthy and hypercaloric meals. Herein we have hypothesized that chronic feeding with chicken fat and fructose, together or by separate, can cause pulmonary redox and inflammatory changes. These changes are particularly related to neutrophils and myeloperoxidase, with consequent changes in the organ histophysiology. To test this hypothesis, we fed mice for 16 weeks with either control food (low-fat diet, LFD) or control food supplemented with 22% chicken fat and with or without 10% fructose in the drinking water. At the end of the feeding regimen, we measured redox and inflammatory changes in the lung with particular emphasis on neutrophil accumulation/activation and molecular-histological markers of fibrosis. Our results suggest that a diet supplemented with chicken fat and fructose causes additive effects on pulmonary oxidative stress, inflammation, and a pro-fibrotic status. Neutrophilic inflammation may play a critical role in pulmonary pathology associated with metabolic syndrome.

**KEY WORDS:** diet; metabolic syndrome; neutrophilic inflammation; myeloperoxidase; incipient lung fibrosis.

**Electronic supplementary material** The online version of this article (https://doi.org/10.1007/s10753-019-01051-9) contains supplementary material, which is available to authorized users.

[1] Laboratory of Experimental and Translational Medicine, Multidisciplinary Institute of Biological Research-San Luis, IMIBIO-SL, CONICET, National University of San Luis, Suite 13X, First Floor, Chacabuco 917, 5700 San Luis, San Luis, Argentina
[2] Laboratory of Experimental Therapeutics and Nutrition, IMIBIO-SL, CONICET, National University of San Luis, 5700 San Luis, San Luis, Argentina
[3] Laboratory of Molecular Biology, IMIBIO-SL, CONICET, National University of San Luis, 5700 San Luis, Argentina
[4] LIAM. Andrology Research Laboratory from Mendoza, IHEM-CCT, Mendoza-National University of Cuyo, 5500 Mendoza, Mendoza, Argentina
[5] Laboratory of Anatomophophysiology, IMIBIO-SL, CONICET, National University of San Luis, 5700 San Luis, San Luis, Argentina
[6] To whom correspondence should be addressed at Laboratory of Experimental and Translational Medicine, Multidisciplinary Institute of Biological Research-San Luis, IMIBIO-SL, CONICET, National University of San Luis, Suite 13X, First Floor, Chacabuco 917, 5700 San Luis, San Luis, Argentina. E-mails: sandraegomezmejiba@yahoo.com; ramirezlabimibiosl@ymail.com

**Abbreviations:** BALF, Bronchoalveolar lavage fluid; ECM, Extracellular matrix; HFD, High-fat diet; iNOS, Inducible nitric oxide synthase; ICAM-1, Intercellular adhesion molecule-1; LFD, Low-fat diet; NOX, NAPDH-dependent oxido-reductase; MDA, Malondialdehyde; TBARS, Tiobarbituric acid-reactive substances; GSH, Reduced glutathione; GSSG, Oxidized glutathione; SOD, Superoxide dismutase; CAT, Catalase; GPx, Glutathione peroxidase; MMP, Metalloproteinase; MPO, Myeloperoxidase; MS, Metabolic syndrome: RT-PCR; Reverse transcriptase-polymerase chain reaction; TAC, Total antioxidant capacity

## INTRODUCTION

Worldwide, obesity is increasing and contributing to the overall burden of chronic diseases [1]. The combination of chicken fat in the food and fructose (10–15%) in the drinking water, as observed in the American diet, has been linked to an increased incidence of metabolic syndrome (MS). This syndrome includes insulin resistance, dyslipidemia, hypertension, and liver steatosis. This constellation of diseases is a consequence of systemic oxidative stress and inflammation resulting from either an inflamed adipose tissue by-product of the metabolism or directly from the diet [2].

In obese patients, fat distribution appears to be an important contributing factor to morbidity and healthy survival [3]. Especially an increase in visceral fat is associated with diabetes and other metabolic abnormalities associated with obesity [4, 5].

In recent years, a positive relationship has been found between lung function impairment and features of the metabolic syndrome, predominantly visceral adiposity in view of the major role of inflammation in lung function impairment [6]. In addition to the physiologic effects of obesity on lung function, several investigators have hypothesized that obesity leads to a state of low-grade systemic inflammation that may affect the lung [7]. Such an association, though speculative, is surprising because obesity is believed to be an inflammatory state with mild baseline elevations in the blood of TNF-α, IL-1β, IL-6, and IL-8, as well as increased blood neutrophil content [8–10]. Alveolar recruitment of neutrophils is thought to be a central player in the onset and progression of lung inflammation [10]. Increases in alveolar airspace neutrophilia and plasma myeloperoxidase (MPO) and inflammatory cytokine concentration, including TNF-α, IL-1β, IL-6, and IL-8, are associated with increased morbidity and mortality in obesity [11, 12].

Several studies have shown that in obesity, there are more activated leukocytes in the peripheral circulation [13, 14]. An human adult has a cardiac output of 5 l of blood/min, in 24 h, and pumps approximately 7200 l of blood through the pulmonary circulation. The diameter of the pulmonary capillaries is smaller (7 μm) than the diameter of the neutrophils (9–12 μm), which forces the neutrophils to deform in the vascular system [15]. Therefore, the movement of neutrophils in the pulmonary vessels is one of the slowest relative to other blood vessels. The lung is a sink of neutrophils because it contains 30-fold more neutrophils than any other major blood vessel [16]. These properties of the pulmonary microcirculation make the lung an important reservoir of neutrophils, and at the same time highly susceptible to small redox/inflammatory changes in the systemic compartment in obesity [17].

Among the factors capable of stimulating extracellular matrix (ECM) production, TGF-β is considered the "*redox-sensitive master switch*" for lung fibrosis [18]. It also acts *via* matrix metalloproteinases (MMPs) and upregulation of matrix-binding integrins, which in turn can activate TGF-β therefore promoting the production of fibrillar collagens, among other ECM proteins. Interestingly, TGF-β represents the best example of redox-dependent growth factor-induced EMC expression because many of its pro-fibrotic effects are dependent on NADPH oxidase-4 (NOX-4) and the generation of reactive species [19].

Previously, we have developed a mouse model displaying many of the characteristics of human metabolic syndrome. However, to our knowledge, there are no studies linking chronic feeding with food supplemented with chicken fat and fructose on lung redox and inflammatory status and possible consequences on lung fibrosis. The objective of this work was to determine the effect of chronic feeding of mice with food supplemented with chicken fat and fructose in the drinking water on the pulmonary redox and inflammatory profile and possible pro-fibrotic mechanisms and consequences.

## MATERIALS AND METHODS

### Animals

Male C57BL/6J mice weighing approximately 20 g (6 weeks-old) were housed and fed in the Animal Care Center of National University of San Luis (San Luis, Argentina). Mice were kept under controlled conditions with a temperature of 24 ± 2 °C and a 12-h light-12-h dark cycle and free access to food and water. Groups of six animals per group were used for the experimental procedure. All experiments and procedures are performed in compliance with the Manual on Care and Use of Laboratory Animals published by the US National Institute of Health. All experimental procedures used in this study were approved by the Institutional Animal Care and Use Committees of the National University of San Luis (protocol no. B97/15).

### Experimental Procedures

The animals were randomly divided in the four groups: low-fat diet (LFD or control), low-fat diet with fructose (10%) (ENA Sports, Buenos Aires, Argentina) in drinking water (LFD + F), high-fat diet (HFD), and high-fat diet with fructose (10%) in drinking water (HFD + F). Each experimental group was *ad libitum* fed with these diets for 16 weeks. The control group (LFD) was fed with a purified-rodent diet (GEPSA, Pilar Group S.A., Buenos Aires, Argentina), whereas the high-fat diet the purified-rodent diet with the addition of 22% chicken fat (Granja Tres Arroyos, Buenos Aires, Argentina). The body weight of the animals was weekly monitored. Systolic blood pressure (SBP) was measured during the entire 16 weeks of feeding with a noninvasive tail-cuff system by using a CODA Surgical Monitor (Kent Scientific Co.). Measurements were performed and presented according to the manufacturer's instructions. To analyze basal blood glucose levels, mice have fasted for 12 h [2].

At the end of these measurements, animals were lightly anesthetized with vapors of isoflurane and then were sacrificed by cervical dislocation. Subsequently, thoracotomy was performed, the trachea was exposed, and the lung was lavaged twice using 0.5 ml PBS. The bronchoalveolar lavage fluid (BALF) was centrifuged at 1000 rpm (433 × *g*) for 10 min at 4 °C. The resulting pellet was suspended in PBS, and differential cytology was performed after staining with Giemsa using a Leica microscope (Leica, Germany) with a magnification of × 100. Each slice was selected for each mouse, and 100 cells were randomly selected from four regions to record the cell count. After lung lavages, lung's right lobe and epididymal fat were collected, weighed, and frozen (− 80 °C) for further analysis. The adiposity index was determined by the ratio: [(epididymal fat / final body weight) × 100] [20]. The left lung's lobe was kept in 10% formalin for a histopathology examination.

### Staining and Histology

For the histological study, the left lung lobe of three mice per group was excised, and the samples were immersed in the fixative (Bouin's solution) for 2 h. The samples were dehydrated and then embedded in paraffin. Subsequently, sections of 5–6 μm thickness were obtained with a Porter Blum Hn40 microtome. Histological sections were dewaxed, hydrated, and stained with hematoxylin-eosin (H&E) or Masson's trichromic. After mounting, pictures were acquired with a Leitz optical microscope equipped with a Leica camera (image magnifications of × 40 and × 100 are shown).

### Preparation of Tissue Homogenates

Six lungs per experimental group were homogenized separately in 200 μl of RIPA buffer (Thermo Fisher Scientific Inc., MA, USA) according to the manufacturer's instructions. Tissue homogenates were centrifuged at 14,000 × *g* for 15 min at 4 °C to remove the nuclei and cell debris. The total protein concentration in tissue homogenates was measured by the Bradford method, using bovine serum albumin as a standard [21].

### Hydroxyproline Measurement in Lung Homogenates

Hydroxyproline content was determined in lung tissue as marker of fibrosis following a previously published method [22]. Briefly, the homogenized lung samples (100 mg) were homogenized in 300 μl of RIPA buffer, and then they were dried in a 110 °C oven for 48 h. After acid hydrolysis, vials were incubated under anoxic conditions for 24 h at 110 °C. The vials were then broken, and the acid was allowed to evaporate for 24 h at 110 °C. Samples were reconstituted with 2 ml of sterile saline, sealed with parafilm, incubated for 1 h in 60 °C, and then centrifuged. The supernatants were analyzed for hydroxyproline. The processed tissue samples were incubated with 0.5 ml of chloramine-T solution for 20 min at room temperature, followed by addition of 0.5 ml of 3.15 M perchloric acid and incubation for 5 min at room temperature. Next, 0.5 ml of p-dimethylaminobenzaldehyde solution was added and incubated for 20 min at 60 °C for color development. The samples were read in a 96-well plate at 557 nm in a plate reader. Hydroxyproline content is shown as $OD_{557nm}$/100 mg tissue.

### Total Antioxidant Capacity in Lung Homogenates

Total antioxidant capacity (TAC) was measured by an improved method of quenching of the 2,2′-azino-bis-(3-ethylbenzothiazoline-6-sulfonic acid) radical cation ($ABTS^{\bullet+}$) by both lipophilic and hydrophilic antioxidants present in the lung homogenates [23].

### Antioxidant Enzyme Activity in Lung Homogenates

Catalase (CAT) activity was determined by measuring the decrease in absorption at 240 nm in a reaction medium containing 50 mM phosphate buffer (pH 7.3) and 3 mM $H_2O_2$ [24]. Glutathione peroxidase (GPx) activity was determined following NADPH oxidation at 340 nm in a

reaction medium containing 0.2 mM GSH, 0.25 IU/ml yeast glutathione reductase, 0.5 mM and *tert*-butyl hydroperoxide (Sigma Chemical Co. St. Louis, MO), and 50 mM phosphate buffer (pH 7.2) [25]. Copper-zinc superoxide dismutase (CuZn-SOD) activity was determined on the basis of its inhibitory action on the rate of superoxide-dependent reduction of cytochrome c by xanthine-xanthine oxidase at 560 nm. The reaction medium contained 50 mM phosphate buffer (pH 7.8), 50 mM xanthine, 20 mM cytochrome c, and xanthine oxidase (Sigma Chemical Co.), to change 0.025 units/min absorbance [26].

### Measurement of Oxidative Stress Markers in Lung Homogenates

As a marker of protein oxidation, protein carbonyls were determined as previously reported using an enzyme-linked immune-sorbent assay (ELISA) and the results are shown as nanomoles of carbonyl per milligram of total proteins (nmol/mg protein) [27]. Lipid peroxidation was measured spectrophotometrically by determining malondialdehyde (MDA) concentration as thiobarbituric acid-reactive substances (TBARS) at 535 nm, and results are shown as micromoles of MDA per milligram of total proteins (μmol MDA/mg protein) [28]. As a marker of nitrosative stress, protein nitration was determined using an ELISA. The primary antibody against nitrotyrosine was produced in our laboratory (1/1000 dilution in washing buffer). A standard curve was created with serial dilutions of nitrotyrosine-BSA, and the results are shown as μmol/mg protein [29]. Chlorotyrosine—a biomarker of HOCl-induced protein oxidation—was determined using an ELISA with an antibody anti-3-chlorotyrosine (1/1000; cat. no. 428035, MERK MILLIPORE, Billerica, MA). The secondary antibody anti-rabbit IgG-HRP conjugate (1/10,000 in washing buffer) and the oxidation of the HRP substrate 3,3′,5,5′-tetramethylbenzidine (TMB) were read at 450 nm using a TECAN microplate reader (Infinite M200 PRO, Research Triangle Park, NC).

### GSH/GSSG Ratio

Glutathione is the main intracellular low-molecular-weight thiol which plays a critical role in cell defense against oxidative stress in cells and tissues. Concentrations were measured in lung homogenate using a commercial kit following manufacturer instructions (cat. no. K264–100, BioVision Inc., Milpitas, CA) [30].

### Determination of TNF-α

Following homogenization of the pulmonary tissues, the cytokine protein concentrations were measured using a mouse TNF-α DuoSet ELISA Kit (cat. no. DY410, R&D Systems, Minneapolis, MN) following the instructions provided by the manufacturer [31].

### Myeloperoxidase Activity Assay

Tissue was re-suspended in 1 ml of 50 mM phosphate buffer (pH 6.0) containing 0.5% hexadecyltrimethylammonium bromide (HTA-Br) and then homogenized. The homogenate was frozen and thawed and then centrifuged at 12,000 × *g* for 10 min. An assay mixture was prepared to contain 0.1 ml supernatant; 2.9 ml buffer containing 0.19 mg/ml o-dianisidine chloride, and reaction was started with the addition of 0.0005% $H_2O_2$ as substrate and was read on a spectrophotometer (TECAN Infinite M200 PRO microplate reader, Research Triangle Park, NC) at 460 nm for 2 min at the interval of 30 s. MPO activity was calculated as a change in absorbance/min/mg protein [32].

### RNA Isolation and Reverse Transcriptase Reaction

Total RNA was extracted from lung tissue from four mice per experimental group. Every RNA isolation was performed using Quick-zol reagent (Kalium Technologies, Buenos Aires, Argentina) as suggested by the manufacturers. Gel electrophoresis and Gel Red™ nucleic acid gel stain (Biotium Inc., San Francisco, CA) was used to confirm the integrity of the samples. Total RNA was reverse transcribed at 42 °C with 200 units of M-MLV Reverse Transcriptase (PB-L Productos Biológicos, Buenos Aires, Argentina) to produce cDNA by following the manufacturer's instructions.

### Polymerase Chain Reaction

Transcript concentration of CAT, GPx, SOD, MPO, NOX-2/4, ICAM-1(intercellular adhesion molecule), IL-6 (interleukin 6), iNOS (inducible nitric oxide synthase), TGF-β1, and MMP-9 were determined by reverse transcriptase-polymerase chain reaction (RT-PCR) and normalized to β-actin as a housekeeping gene. Fragments coding for these genes were amplified by PCR in a 20 ml reaction-solution mix containing 0.2 mM dNTPs, 1.5 mM $MgCl_2$, 1 IU of Taq polymerase, and 10 μmol of each mouse-specific oligonucleotide primer and RT-generated cDNA (1/10 of RT reaction). Nucleotide sequences of the specific primers are shown in Supplementary Table 1.

cDNA amplification was performed using a thermocycler (MyCycler; BioRad Laboratories, Inc., Hercules, CA). The reaction products were electrophoresed on 2% agarose gels, visualized with GelRed™ (0.05 ml/ml), and examined by ultraviolet transillumination. Band intensities of RT-PCR amplicons were quantified using ImageJ (Image Processing and Analysis in Java from http://rsb.info.nih.gov/ij/). Relative levels of mRNA were expressed as the ratio between the signal intensity of target genes and that for the housekeeping gene.

### Immunofluorescence

For staining of tissue sections, murine lung tissue was fixed in 4% formalin prior to paraffin embedding. Three-micron sections were prepared and mounted on slides, followed by deparaffinization and immunofluorescent staining according to a standard protocol. Primary antibodies used were mouse monoclonal anti-NIMP-14 (Hycult Biotech, cat. no. HM1039The Netherlands 1:200). Secondary antibodies were goat anti-rat F(ab′)2 Anti-Rat IgG-H&L(FITC) antibody (Abcam, cat. no. ab6242, Cambridge, UK, 1:5000). The nuclei were stained with DAPI (Thermo Scientific, Massachusetts, EEUU, 1:1000) for 10 min in darkness. Then, the slides were examined using a Nikon Microscope. Green fluorescence was quantified by using the ImageJ software [33]. For each image, data are shown as relative units of immunofluorescence (IF).

### Statistics

All data are shown mean values ± standard error of the mean (S.E.M.) for each group. Statistical analysis was performed using GraphPad Prism, and the data were analyzed by one-way analysis of variance (ANOVA) followed by the Bonferroni *post hoc* test. A difference was considered to be statistically significant when $p < 0.05$.

## RESULTS

### Characteristics of Mice after Chronic Feeding with Chicken Fat and Fructose

Table 1 shows the general characteristics of our mouse model. After 16 weeks of feeding a high- (HFD) or a low-fat (LFD) diet, with or without 10% fructose in the drinking water (LFD + F and HDF + F), those mice feed an HFD + F showed an increased weight gain, epididymal fat weight, adiposity index (AI), fasting blood glucose (FBG), and systolic blood pressure (SBP) as compared to the other experimental groups. Compared to mice fed an LFD, those mice fed chicken fat feeding had increased weight gain, epididymal fat depot, and SBP. Fructose alone (LFD + F) increased SBP in mice as compared to those mice fed an LFD alone. These data clearly show that both chicken fat and fructose contribute to the metabolic syndrome features in the HFD + F group [2].

### Chronic Feeding with Chicken Fat and Fructose Affects Pulmonary Histomorphology and Differential Cytology

Analysis of slides stained with H&E showed that the pulmonary parenchyma of the LFD mouse group had normal histology (Fig. 1a). The lung the parenchyma of the LFD + F group showed a fibrosis-like aspect and some inflammatory cell infiltration (Fig. 1b, *indicated by black arrows*), whereas the histology of the lung of HFD is compatible with an incipient fibrosis pattern (Fig. 1c). The lung of mice from the HFD + F group showed a large leukocyte infiltration and incipient fibrosis, but more generalized than in the HFD group (Fig. 1d). Indeed, Table 2 shows differential cytology of BALF indicating that the HFD + F group had a higher percentage of neutrophils and lymphocytes as compared to the other experimental groups, whereas this group had a lower percentage of macrophages. On the other hand, there was no significant difference in the proportion of macrophages, lymphocytes, and neutrophils between the other experimental groups (Table 2).

### Chronic Feeding with Chicken Fat and Fructose Increases Neutrophilic Infiltration in the Lung

Based on our observation that compared to the other groups the HFD + F group had the highest proportion of leukocytes in BALF, the neutrophil infiltration in the pulmonary parenchyma was investigated by immunofluorescence using the antibody anti-NIMP-14 (Fig. 2a–d, *indicated by white arrows*). Densitometry analysis of anti-NIMP-14 fluorescence distribution is shown in Fig. 2e. Figure 2 a shows the presence of neutrophils in the normal mouse lung parenchyma. Compared to the LFD group, the content of neutrophils was higher in the LFD + F group (Fig. 2b), but similar to the HDF group (Fig. 2c). The parenchyma of the lung of the HFD + F group had the greatest neutrophil infiltration among all the experimental groups ($p < 0.001$). Of noteworthy, there was no difference in neutrophil content between the HFD and LFD + F groups but were higher than in the LFD group ($p < 0.01$).

**Table 1.** Characteristic of Mice Chronically Fed with Chow Supplemented with Chicken Fat and/or Fructose in the Drinking Water

| | LFD* | LFD + F | HFD | HFD + F |
|---|---|---|---|---|
| Weight (g) | 27.17 ± 0.53 | 28.97 ± 0.79 | 33.18 ± 0.89[b,d] | 36.17 ± 1.37[c,e,f] |
| Epididymal Fat (g) | 0.39 ± 0.02 | 0.66 ± 0.10 | 1.11 ± 0.13[b] | 2.06 ± 0.24[c,e,f] |
| Adiposity Index (IA,%) | 1.44 ± 0.10 | 2.39 ± 0.35 | 3.37 ± 0.42 | 5.82 ± 0.78[c,e,f] |
| FBG (mg/dL) | 110.50 ± 6.87 | 113.50 ± 15.29 | 144.20 ± 15.78 | 181.80 ± 24.00[c] |
| SBP (mmHg) | 142.6 ± 2.5 | 157.4 ± 2.4[a] | 162.3 ± 2.9[b] | 203.0 ± 4.5[c,e,f] |

Statistical symbols indicate $p < 0.05$: a LFD vs LFD + F; b LFD + F vs HFD; c LFD vs HFD + F; d LFD + F vs HFD; e LFD + F vs HFD + F; f HFD vs HFD + F. $n = 6$

*LFD* low-fat diet (6.0% fat, 40.7% carbohydrates and 24% protein), *LFD + F* low-fat diet with fructose in the drinking water, *HFD* high-fat diet (43.77% fat, carbohydrates 22.23% and 20.28% protein), *HFD + F* high-fat diet with fructose in the drinking water, *FBG* fasting blood glucose, *SBP* systolic blood pressure

*Values are shown as mean values ± standard error of the mean (SEM)

Figure 2 e shows a densitometry quantification of the fluorescence intensity of the images shown in Fig. 2a–d.

### Chronic Feeding with Chicken Fat and Fructose Alters Pulmonary Inflammatory and Redox Profile

To evaluate the inflammatory profile of the lung of our experimental groups, we measured the concentration of IL-6 in the BALF by ELISA, and of TNF-α and ICAM-1 by RT-PCR in the lung tissue. Only in the HFD + F experimental group did lung parenchyma homogenates show a significant increase in TNF-α (Fig. 3a), IL-6 (Fig. 3b), and ICAM-1 (Fig. 3c).

To evaluate the pulmonary's redox profile in our mouse model, we measured the source of oxidants (NOX-2, iNOS, and MPO), antioxidants (TAC, some antioxidant enzymes and GSH), and markers of oxidative stress (nitrotyrosine, carbonyls, and lipid peroxidation). We observed an increased content of NOX-2 (Fig. 4a), iNOS (Fig. 4b), and MPO (Fig. 4c) mRNA in the lung tissue of the HFD + F group as compared with the LFD group ($p < 0.05$). MPO activity also increased in the group

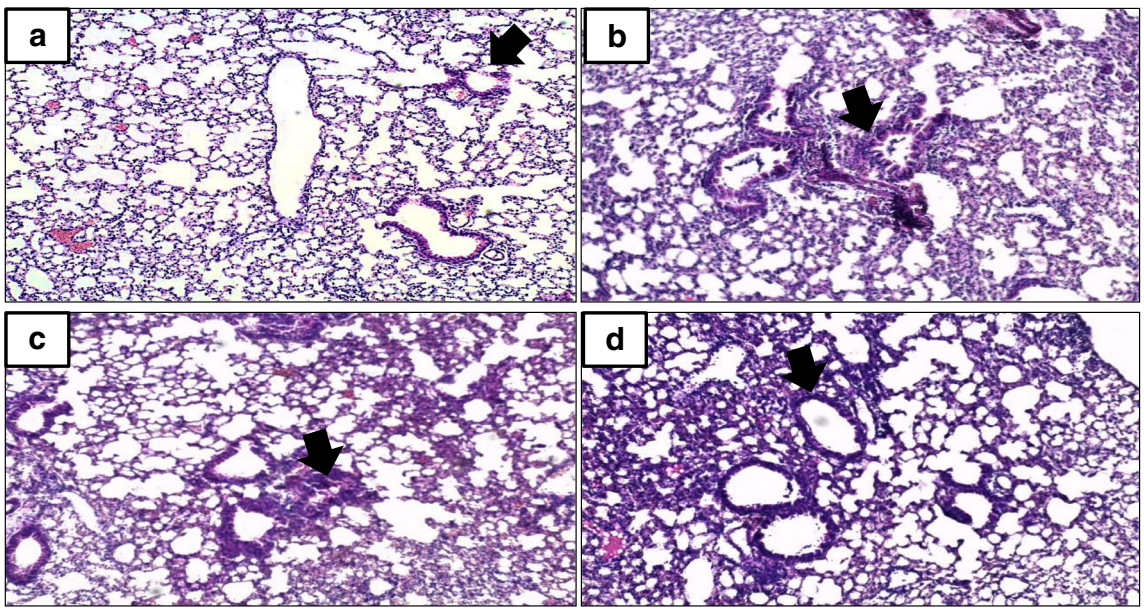


**Fig. 1.** Lung histology in mice chronically fed with chow supplemented with chicken fat and fructose in the drinking water. Representative photograph of H&E staining (× 100) of lung sections from each group of animals after 16 weeks of feeding with **a** LFD, **b** LFD + F, **c** HFD, and **d** HFD + F. The black arrow indicates inflammation and fibrosis. Light incipient fibrosis and inflammatory involvement were observed in the LFD + F and HFD group, while in the HFD + F group, there was increased leukocyte infiltration and generalized incipient fibrosis. A representative H&E image is shown for each group ($n = 4$/group).

**Table 2.** Differential Cytology of BALF from Mice Fed a Diet Supplemented with Chicken Fat and/or Fructose

| | LFD* | LFD + F | HFD | HFD + F |
|---|---|---|---|---|
| Macrophages (%) | 95.0 ± 1.9 | 90.0 ± 1.3 | 85.0 ± 0.9[b] | 80.0 ± 1.0[c] |
| Lymphocytes (%) | 5.0 ± 0.1 | 5.0 ± 0.8 | 10.0 ± 0.4[b] | 10.0 ± 0.2[c] |
| Neutrophils (%) | – | 5.0 ± 0.2 | 5.0 ± 0.2 | 10.0 ± 0.5 |

*Values are shown as mean values ± S.E.M. of cell type as percentages of cells found in BALF. n=6. LFD low-fat diet (6.0%fat, 40.7% carbohydrates and 24%protein), LFD + F low-fat diet with fructose in the drinking water, HFD high-fat diet (43.77%fat,carbohydrates 22.23% and 20.28% protein), HFD+ F high-fat diet with fructose in the drinking water.
Statistical symbols indicate $p < 0.05$: b LFD+F vs HFD; c LFD vs HFD+F.

HFD + F as compared to the LFD group and the other experimental groups (Fig. 4d). No difference in these parameters was observed between the LFD + F and the other experimental groups.

Redox profile in the lung of our experimental groups is shown in Table 3. Compared to LFD group, the lung of HFD + F group had a decreased TAC ($p < 0.01$), a decreased GSH/GSSG ratio ($p < 0.05$), but an increased SOD, CAT, and GPx ($p < 0.001$) specific activity (Table 3). Compared to LFD, chicken fat feeding caused a reduced pulmonary GSH/GSSG ratio, but an increased GPx activity ($p < 0$, 01), whereas fructose in the drinking water (LFD + F) caused an increased pulmonary GPx activity ($p < 0.05$). These data were corroborated by analyzing mRNA expression for these enzymes (Supplementary Fig. 1).

As markers of oxidative stress, lipid peroxidation, carbonyls, nitrotyrosine, and chlorotyrosine were measured. The concentration of TBARS—a marker of lipid peroxidation($p < 0.001$), carbonyls—a marker of protein oxidation, nitrotyrosine—a marker of nitrosative stress($p < 0.05$), and chlorotyrosine—a marker of MPO activation were increased in the HFD + F group as compared to the other experimental groups. As compared to LFD, feeding the mice with chicken fat (HFD) increased TBARS, nitrotyrosine, and chlorotyrosine, whereas fructose in the drinking water caused only increased pulmonary chlorotyrosine content.

### Chronic Feeding with Chicken Fat and Fructose Contribute to Incipient Pulmonary Fibrosis

Loss of metabolic homeostasis and chronic low-grade inflammation appear to play a role in the pathogenesis of fibrosis [34]. To assess the fibrotic status of the lung parenchyma, we stained pulmonary slides with Masson's trichromic stain and determined the expression of molecular markers of fibrosis (MMP-9, TGF-β1, and NOX-4). The images of the trichromic staining are shown at a magnification of × 40 and × 100. Microscopic analysis of lung tissue section stained with Masson's trichromic stain shows in the LFD group (Fig. 5a) the presence of a small amount of sub-epithelial connective tissue in the bronchial tree or in the vascular walls. In the parenchyma, insignificant fibroblastic activity is observed. In the LFD + F lung (Fig. 5b, *indicated by black arrows*), the presence of a moderate amount of sub-epithelial connective tissue is observed in the bronchial tree or in the vascular walls. In the stroma, there is a slight fibroblastic activity that may increase the production of collagen fibers. In addition, there are small areas of cellular infiltration of the stroma. In the HFD lung (Fig. 5c), the sub-epithelial connective is observed in normal amounts, the presence of connective at the level of the bronchial tree or in the vascular walls is observed, but neither in the stroma nor in the bronchial space cell infiltration present is observed. In the lung of HFD + F (Fig. 5d) mice, the increased deposit of extracellular fibrillar sub-epithelial matrix (connective tissue) is seen in blue. It can be observed that there is collagen production in the cells of the matrix as shown by the blue background between the cells of the matrix. In addition, there is certain disorganization of the matrix with strong cellular infiltration around the bronchial tree. Collagen deposition in the lung tissue as shown in Fig. 5a–d, at × 40 magnification, was measured and data are shown in Fig. 5e as % of positive trichromic areas. The greatest deposition of collagen occurred in the lung tissue of HFD + F fed animals, followed by HFD fed animals. In addition, hydroxyproline content in the lung tissue is shown in Fig. 5f. Although we could not find differences in hydroxyproline content, there is a tendency towards an increase, thus resembling the pattern shown in collagen deposition shown in Fig. 5e. Trichromic staining and hydroxyproline content in the lung tissue suggests that chronic consumption of a diet supplemented with chicken fat and fructose cause incipient fibrosis in the mouse lung.

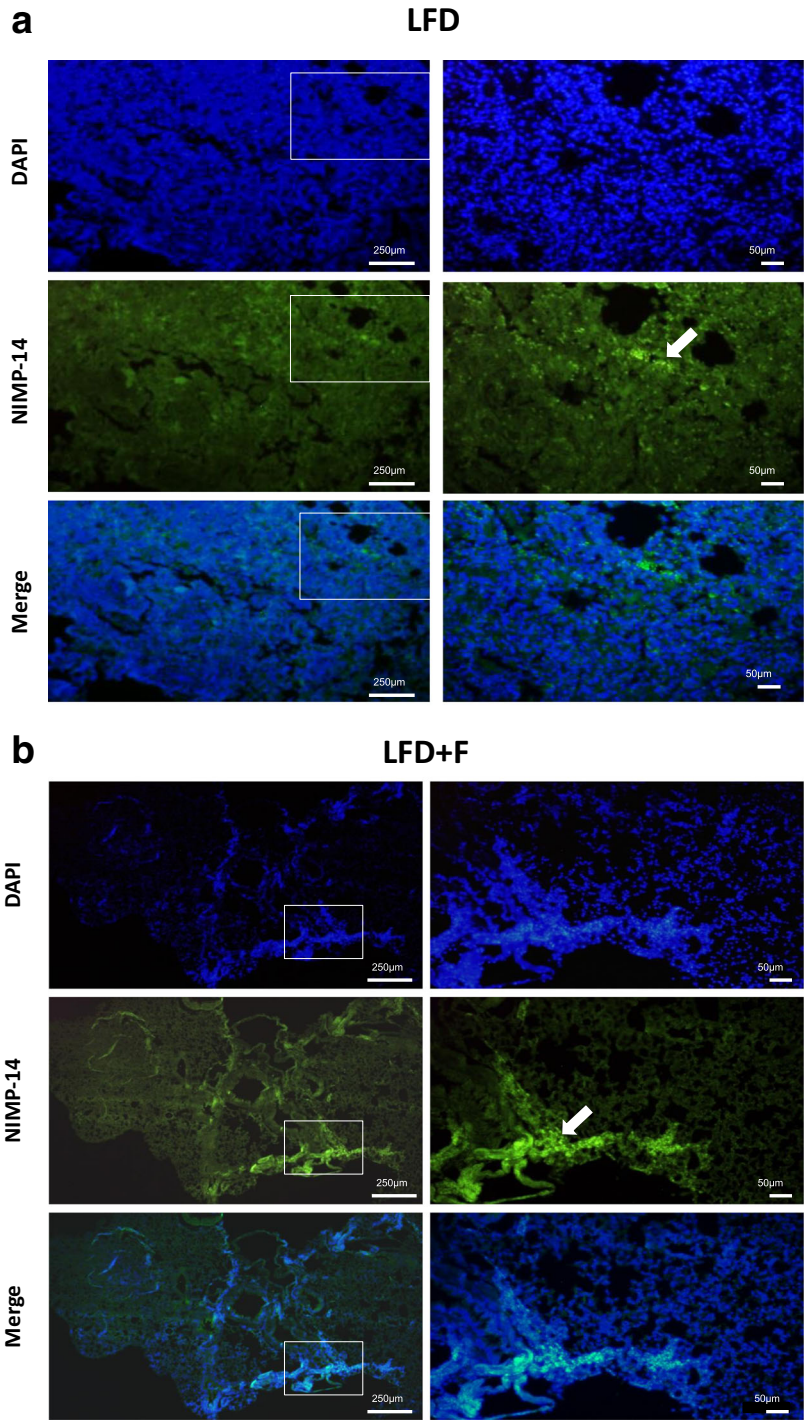


**Fig. 2.** Neutrophil homing in the lung parenchyma of mice chronically fed with a diet supplemented with chicken fat and fructose in drinking water. Infiltration of neutrophils in lung tissue was assessed by immunofluorescence in lung sections. **a** LFD. **b** LFD. **c** HFD. **d** HFD + F. White arrows indicate neutrophilic infiltration. Lung tissue was double-labeled with NIMP-14 antibodies (green) to identify neutrophils or with DAPI (blue) to identify the nucleus. Scale bar 50 µm. **e** Relative quantification of green fluorescence intensity (IF). Data are shown as mean values ± SEM and were analyzed using one-way ANOVA followed by Bonferroni post-test. A $p < 0.05$ indicates statistically significant differences. Statistic symbols: *a*, LFD *vs* LFD + F; *b*, LFD *vs* HFD; *c*, LFD *vs* HFD + F; *e*, LFD + F *vs* HFD + F; *f*, HFD *vs* HFD + F. $n = 3$.

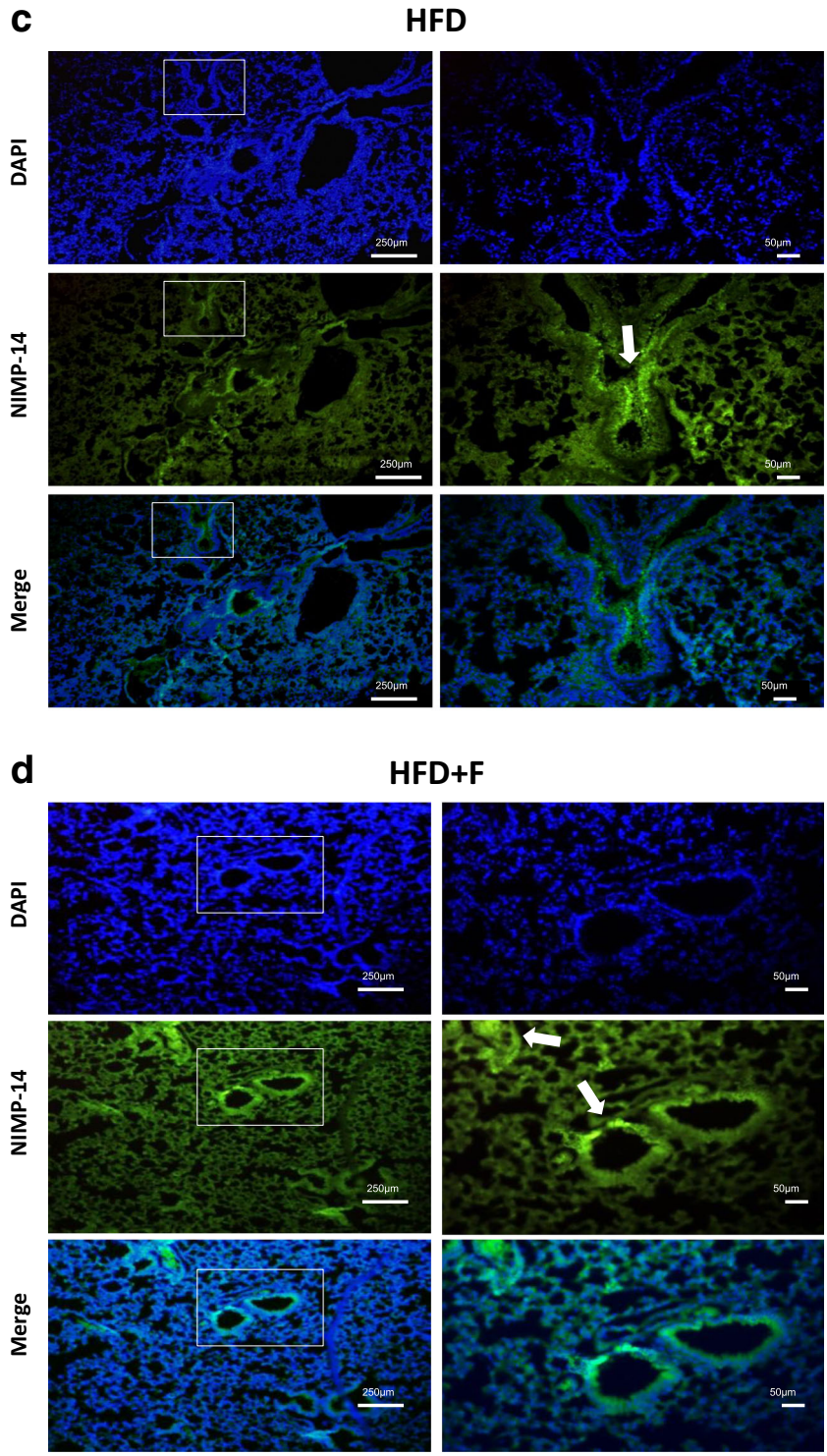


**Fig. 2.** (continued)

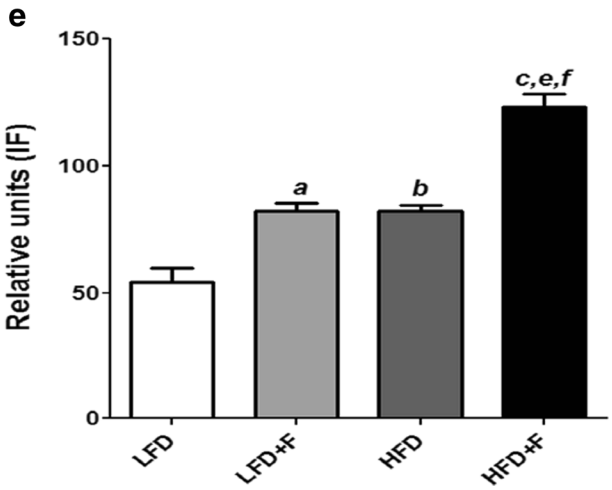


**Fig. 2.** (continued)

Compared to the lung of the LFD group, the pulmonary expression of molecular signatures of fibrosis, both chicken fat and fructose (HFD + F), can trigger increased expression ($p < 0.05$) of MMP-9 (Fig. 6a) and TGF-β1 mRNA (Fig. 6b). NOX-4 expression (Fig. 6c) was not different among the compared experimental groups.

## DISCUSSION

Herein, we show for the first time that chronic feeding with a diet supplemented with chicken fat and fructose caused pulmonary redox/inflammatory changes and a pro-fibrotic status in mice. These pulmonary changes are related to neutrophilic inflammation, which includes increased neutrophil infiltration, MPO activation, and protein chlorination.

Several studies have shown that abdominal obesity may be somehow related to the association between MS and changes in lung physiology [1, 35, 36]. However, the explanation for this relationship is complex but may result from the mechanical and/or metabolic effect exerted by the inflamed adipose tissue on the lung [37].

Adipose tissue is an active endocrine organ that can produce adipocytokines with proinflammatory properties, which then can enter the peripheral circulation to contribute to systemic inflammation [14, 38]. Our data suggest a critical role for adiposity in the relationship between systemic inflammation and neutrophilic inflammation/incipient fibrosis in the lung. Indeed, the transcription of the *IL-6*, *iNOS*, *ICAM-1*, *MMP-9*, and *TGFβ* genes is regulated by the NF-κB signaling pathway, which can be activated by redox changes and TNF-α [36, 39]. The promoter region of the ICAM-1 gene has response elements for several transcription factors (*e.g.*, NF-κB and AP-1) and have also a response element for TNF-α, which in turn is strongly associated with airway inflammation [40, 41]. This is consistent with our results, which show that, in relation to the other experimental groups, HFD + F fed animals have the greatest concentration of proinflammatory cytokines at the systemic and lung compartments.

During the migration of the neutrophils throughout the interstitial tissue, the content of azurophil granules is partially released [42]. We determined the degree of activation of neutrophils by measuring

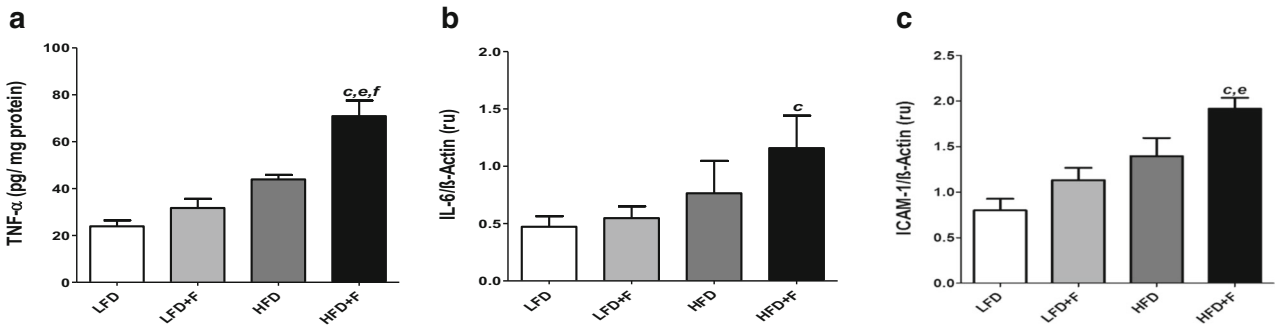


**Fig. 3.** Inflammation markers in the lung of mice chronically fed with chow supplemented with chicken fat and fructose in the drinking water. **a** TNF-α was measured by ELISA in lung homogenates. **b** IL-6, **c** ICAM-1, and β-actin (housekeeping gene) were measured by RT-PCR. Primer sequences are shown in Supplementary Table 1. Values are shown as mean values of absolute concentration or the ratio of band intensities, ± SEM, and were analyzed by one-way ANOVA followed by Bonferroni post-test. Statistical symbols (*c*, LFD *vs* HFD + F; *e*, LFD + F *vs* HFD + F; *f*, HFD *vs* HFD + F) indicate statistical differences ($p < 0.05$). $n = 6$ per experimental group.

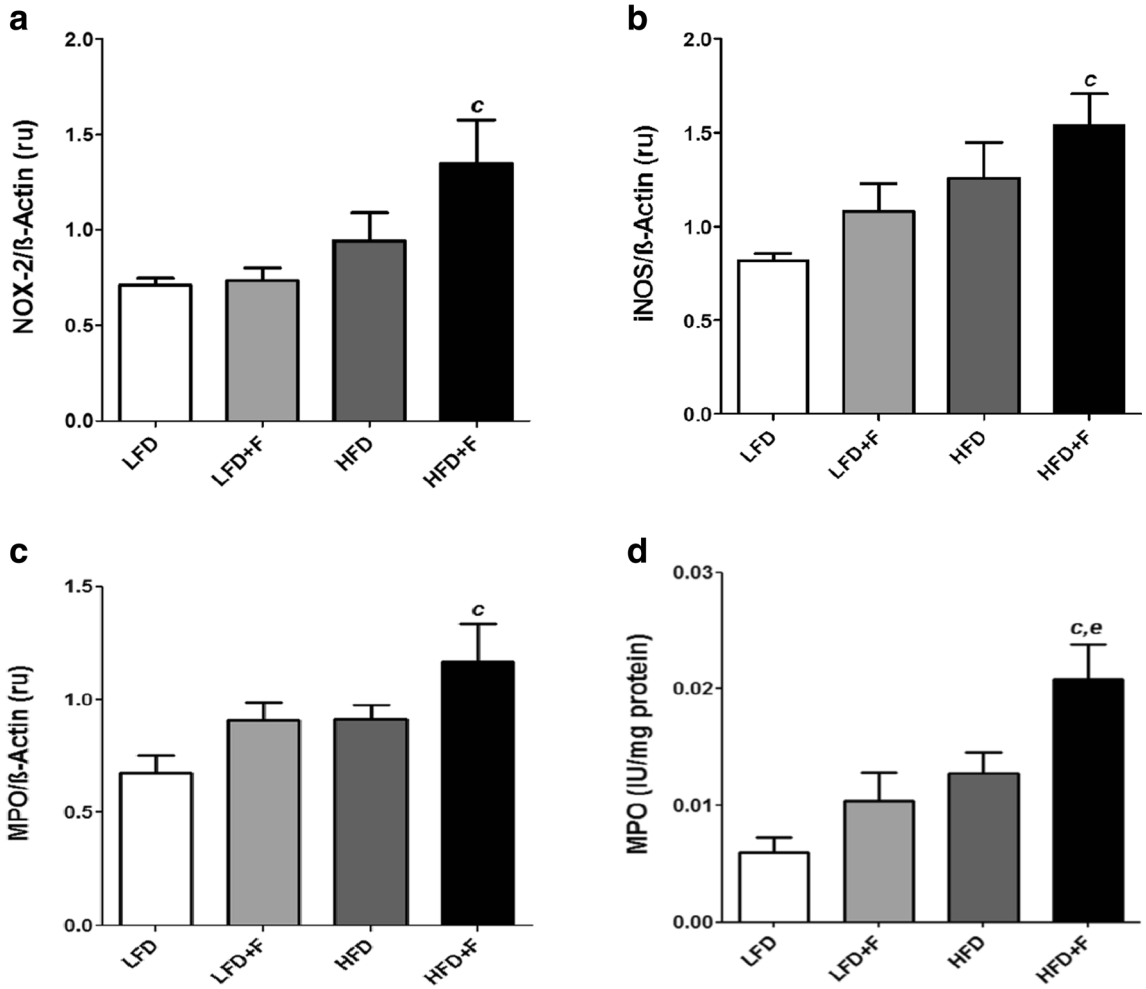


**Fig. 4.** Pulmonary expression and/or activities of enzymes sources of oxidants. **a** NAPDH oxidase-2 (NOX-2). **b** Inducible nitric oxide synthase (iNOS). **c** Myeloperoxidase (MPO) and β-actin (as housekeeping gene) mRNAs were measured by RT-PCR in lung tissue. Band intensities were measured by densitometry using the ImageJ software. Data are shown as the gene of interest-/β-actin- band intensity ratios. **d** MPO activity in lung homogenates was measured using the $H_2O_2$-induced *O*-dianisidine oxidation assay. Data are shown as mean values ± SEM and were analyzed using one-way ANOVA followed by Bonferroni post-test. A $p < 0.05$ indicates differences. Statistic symbols: c, LFD *vs* HFD + F. $n = 6$ per experimental group.

the MPO activity and the chlorination of proteins as an MPO activity fingerprint [41]. Several studies have demonstrated that in morbid obesity, neutrophils are less active [10]. However, we found that the increased infiltration of neutrophils, in the lung parenchyma of animals fed an HFD + F diet, is accompanied by greater activity and expression of MPO. This apparent discrepancy may be due to the uniqueness of our experimental model to induce many of the features observed in the human MS.

NOX-2 is present in the membrane of activated neutrophils and is the most important source of anion radical superoxide ($^{\bullet}O_2^-$) at inflammation sites [43, 44]. One of the functions that $^{\bullet}O_2^-$ fulfills is to maintain active MPO and thereby enhance oxidant damage at inflammatory sites by optimizing the production of HOCl [45, 46]. This agrees with our results, where we found the greater expression of NOX-2, MPO activation, and chlorotyrosine in the lungs of HFD + F fed mice.

The proinflammatory enzyme iNOS is expressed in innate immune cells in response to inflammatory and immune stimuli [47]. In our study, we observed that the lung of HFD + F fed mice overexpresses

**Table 3.** Pulmonary Redox Profile in Mice Chronically Fed with Chow Supplemented with Chicken Fat and/or Fructose in the Drinking Water

| | LFD | LFD + F | HFD | HFD + F |
|---|---|---|---|---|
| *Antioxidants* | | | | |
| TAC (μmol L-ascorbate) | 3263.00 ± 218.80* | 2753.00 ± 205.50 | 2574.00 ± 168.90 | 2106.00 ± 166.30[c] |
| GSH/GSSG ratio | 156.30 ± 9.53 | 134.10 ± 13.79 | 102.70 ± 2.80[b] | 75.66 ± 4.25[c,e] |
| SOD (IU/mg protein) | 10.64 ± 2.48 | 15.72 ± 2.25 | 17.49 ± 3.82 | 33.04 ± 6.12[c,e,f] |
| CAT (IU/mg protein) | 160.60 ± 32.21 | 215.50 ± 31.19 | 230.1 ± 33.99 | 320.90 ± 32.52[c] |
| GPX (IU/mg protein) | 0.39 ± 0.02 | 0.75 ± 0.06[a] | 1.12 ± 0.05b,[d] | 1.55 ± 0.09[c,e,f] |
| *Oxidative stress biomarkers* | | | | |
| TBARS (μmol/mg protein) | 0.44 ± 0.04 | 0.75 ± 0.09 | 1.63 ± 0.15b,[d] | 3.30 ± 0.29[c,e,f] |
| Carbonyls (nmol/mg protein) | 23.64 ± 2.37 | 29.58 ± 1.00 | 31.16 ± 2.68 | 35.75 ± 1.52[c] |
| Nitrotyrosine (μmol/mg protein) | 0.42 ± 0.024 | 0.49 ± 0.02 | 0.64 ± 0.02b,[d] | 1.25 ± 0.09[c,e,f] |
| Chlorotyrosine (fold change) | 0.70 ± 0.02 | 0.86 ± 0.02[a] | 0.95 ± 0.03[b] | 1.13 ± 0.02[c,e,f] |

*LFD* low-fat diet, *LFD + F* low-fat diet with fructose in the drinking water, *HFD* high-fat diet, *HFD + F* high-fat diet with fructose in the drinking water, *TAC* total antioxidant capacity, *TBARS* thiobarbituric acid-reactive substances, *CAT* catalase, *GPx* glutathione peroxidase, *SOD* superoxide dismutase

*Values are shown as mean ± SEM and were analyzed by one-way ANOVA followed by Bonferroni post-test ($p < 0.05$). Statistical symbols (a: LFD *vs* LFD + F; b: LFD + F *vs* HFD; c: LFD *vs* HFD + F; d: LFD + F *vs* HFD; e: LFD + F *vs* HFD + F; f: HFD *vs* HFD + F) indicate statistical differences ($n = 6$ per experimental group)

iNOS in comparison with other experimental groups. In turn, this enzyme produces $^{\bullet}NO$ that reacts with $^{\bullet}O_2^-$ producing peroxynitrite—a powerful nitrating agent, which is found in high concentrations at inflammation sites [48–50]. In effect, we found the highest nitration of proteins in the lungs of HFD + F fed mice.

Loss of metabolic homeostasis and chronic low-grade inflammation appear to play new emerging roles in the pathogenesis of fibrosis [34]. Pulmonary fibrosis is characterized by an excessive accumulation of extracellular matrix and remodeling of the lung architecture that may lead to irreversible tissue damage and dysfunction [34, 51]. In our study, we

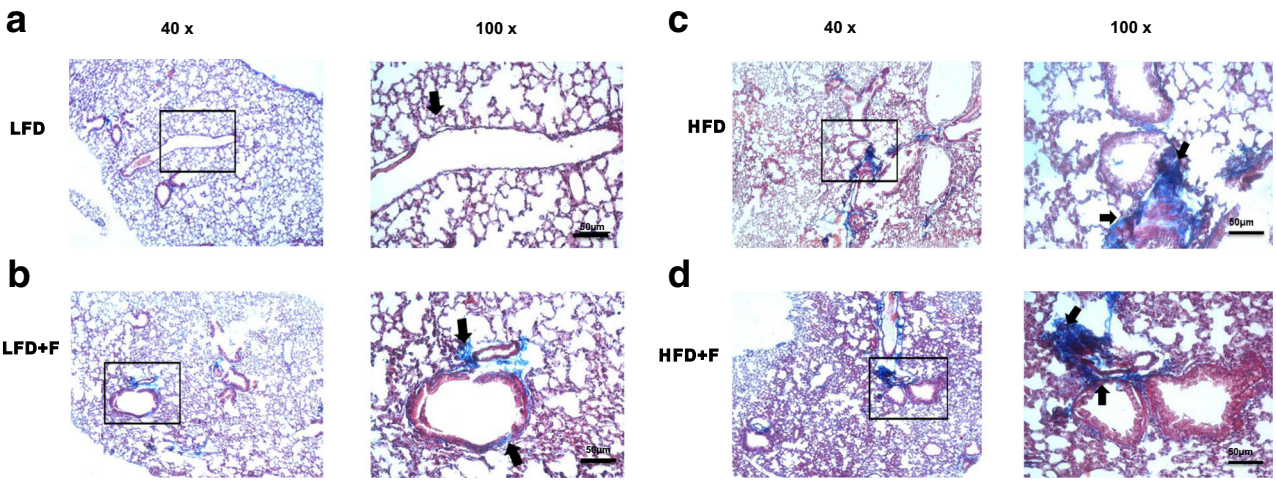


**Fig. 5.** Incipient pulmonary fibrosis in mice chronically fed with chow supplemented with chicken fat and/or fructose in the drinking water. The structures were colored by Masson trichrome in green/blue. Representative images of a lobe section acquired at a magnification of × 40 and at × 100, for each experimental group, are shown. The black arrow indicates an increased deposit of connective tissue (blue color). **a** LFD: The presence of a small amount of connective tissue is observed. **b** LFD + F. **c** HFD: The presence of a moderate amount of sub-epithelial connective tissue is observed in the bronchial tree or in the vascular walls. **d** HFD + F: It is observed collagen production in the matrix (blue background). In addition, certain disorganization of the matrix with strong cellular infiltration around the bronchial tree is observed. **e** Measurement of the area covered by collagen in the images acquired at × 40 as shown in **a**–**d**. **f** Measurement of hydroxyproline content as a marker of collagen synthesis in lung tissue. Values are shown as mean ± SEM and were analyzed by one-way ANOVA followed by Bonferroni post-test. The statistical symbols (*b*: LFD + F *vs* HFD; *c*: LFD *vs* HFD + F; *e*: LFD + F *vs* HFD + F; *f*: HFD *vs* HFD + F) indicate statistical differences at $p < 0.05$. $n = 4$ per experimental group.

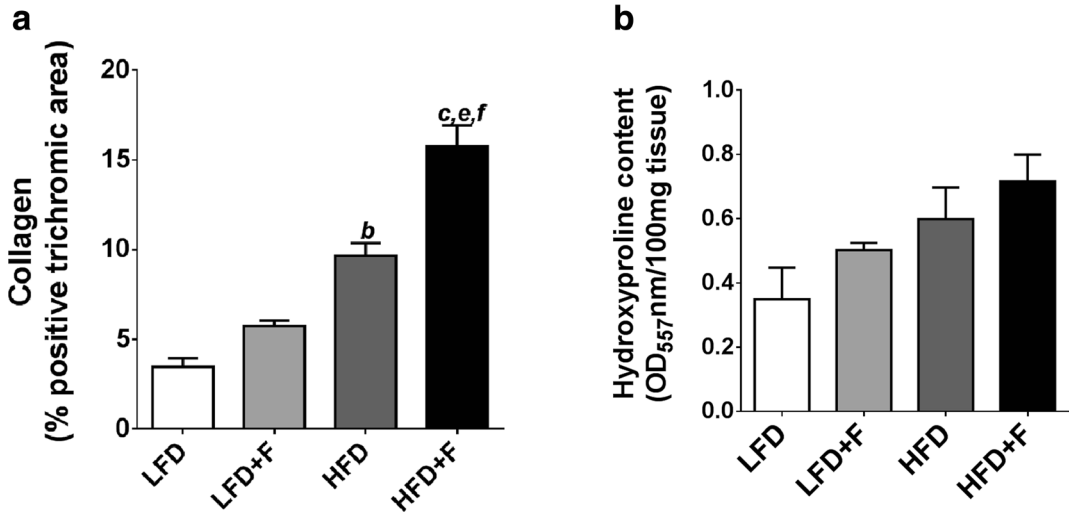


**Fig. 5.** (continued)

observed an increase in the formation of collagen fibers in the lung parenchyma of HFD + F fed mice. This observation agrees with the increased expression of molecular markers of fibrosis, TGF-β1 and MMP-9, in their lungs. In addition to enhanced ROS level, TGF-β1 appears to be a key mediator of the fibrotic process because it can induce collagen production [34]. TGF-β acts *via* MMP-9 leading to upregulation of matrix-binding integrins, which in turn can activate TGF-β. Watson *et. al.* [19] proposed that the TGF-β is the best example of redox-dependent growth factor-inducing collagen accumulation because many of its pro-fibrotic effects are redox-dependent. Throughout these activities, TGF-β can promote the proliferation of fibroblasts and production of matrix glycoproteins-like fibrillar collagen.

## CONCLUSIONS

Chronic feeding of mice with a diet supplemented with chicken fat and fructose causes neutrophilic inflammation, oxidative stress, and pro-fibrosis in the lung. A positive relationship between pulmonary MPO activity and chlorotyrosine in the lung of HFD + F fed mice is consistent with neutrophilic inflammation. Further cause-effect studies are needed to assess whether neutrophilic inflammation can be a

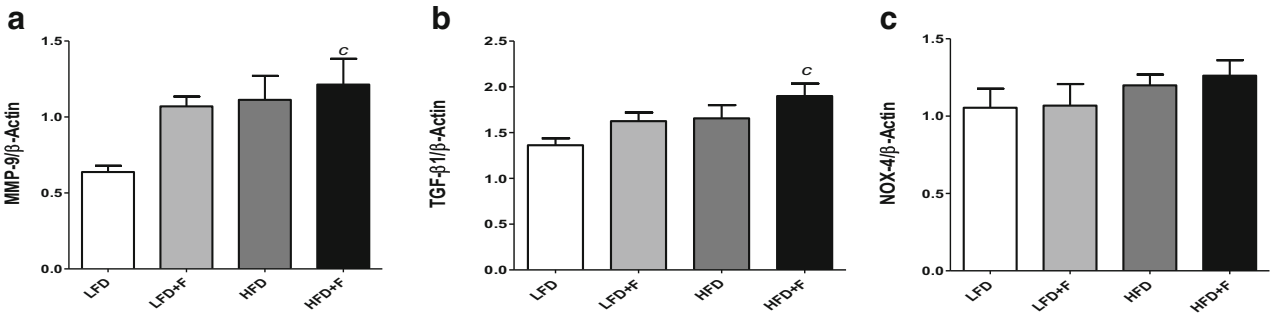


**Fig. 6.** Pulmonary expression of molecular markers of fibrosis in mice chronically fed with chow supplemented with chicken fat plus fructose in the drinking water. RT-PCR measurement of the mRNA encoding for: **a** metalloproteinase 9 (MMP-9), **b** NADPH oxidase-4 (NOX-4), **c** transforming growth factor-beta 1(TGF-β1) and β-actin (housekeeping gene). Primer sequences are shown in Supplementary Table 1. Band intensities were measured using the ImageJ software and shown as the gene of interest/β-actin intensity ratios. Results are shown as mean values ± SEM ($n = 6$). Data were analyzed by using the one-way ANOVA followed by Bonferroni post-test. *c* indicates $p < 0.05$ when comparing LFD *vs* HFD + F.

therapeutic target to prevent pulmonary fibrosis, as well as metabolic abnormalities related to obesity.

## ACKNOWLEDGMENTS

The authors are deeply grateful to the members of the Laboratory of Diabetes, School of Chemistry, Biochemistry and Pharmacy, led by Dr. Susana E. Siewert for helping with gene expression analysis.

Funding informationThis research was supported by the following grants: FONCYT, Argentina (PICT3369, to DCR and SEGM), CONICET, Argentina (PIP916, to DCR and SEGM), and Universidad Nacional de San Luis, Argentina (PROICO2-3418 to DCR; and PROICO, 10-0218 to SEGM).

## REFERENCES

1. Thijs, W., R. Alizadeh Dehnavi, P.S. Hiemstra, A. de Roos, C.F. Melissant, K. Janssen, J.T. Tamsma, and K.F. Rabe. 2014. Association of lung function measurements and visceral fat in men with metabolic syndrome. *Respiratory Medicine* 108: 351–357.
2. Della Vedova, M.C., M.D. Munoz, L.D. Santillan, M.G. Plateo-Pignatari, M.J. Germano, M.E. Rinaldi Tosi, S. Garcia, N.N. Gomez, M.W. Fornes, S.E. Gomez Mejiba, and D.C. Ramirez. 2016. A Mouse Model of Diet-Induced Obesity Resembling Most Features of Human Metabolic Syndrome. *Insights in Nutrition and Metabolism* 9: 93–102.
3. Ulrich, M., A. Petre, N. Youhnovski, F. Promm, M. Schirle, M. Schumm, R.S. Pero, A. Doyle, J. Checkel, H. Kita, et al. 2008. Post-translational tyrosine nitration of eosinophil granule toxins mediated by eosinophil peroxidase. *The Journal of Biological Chemistry* 283: 28629–28640.
4. Fox, C.S., J.M. Massaro, U. Hoffmann, K.M. Pou, P. Maurovich-Horvat, C.Y. Liu, R.S. Vasan, J.M. Murabito, J.B. Meigs, L.A. Cupples, R.B. D'Agostino Sr., and C.J. O'Donnell. 2007. Abdominal visceral and subcutaneous adipose tissue compartments: association with metabolic risk factors in the Framingham Heart Study. *Circulation* 116: 39–48.
5. Oka, R., J. Kobayashi, A. Inazu, K. Yagi, S. Miyamoto, M. Sakurai, K. Nakamura, K. Miura, H. Nakagawa, and M. Yamagishi. 2010. Contribution of visceral adiposity and insulin resistance to metabolic risk factors in Japanese men. *Metabolism* 59: 748–754.
6. Broekhuizen, R., E.F. Wouters, E.C. Creutzberg, and A.M. Schols. 2006. Raised CRP levels mark metabolic and functional impairment in advanced COPD. *Thorax* 61: 17–22.
7. Shore, S.A. 2008. Obesity and asthma: possible mechanisms. *The Journal of Allergy and Clinical Immunology* 121: 1087–1093 quiz 1094-1085.
8. Desai, M.Y., D. Dalal, R.D. Santos, J.A. Carvalho, K. Nasir, and R.S. Blumenthal. 2006. Association of body mass index, metabolic syndrome, and leukocyte count. *The American Journal of Cardiology* 97: 835–838.
9. Ramos, E.J., Y. Xu, I. Romanova, F. Middleton, C. Chen, R. Quinn, A. Inui, U. Das, and M.M. Meguid. 2003. Is obesity an inflammatory disease? *Surgery* 134: 329–335.
10. Kordonowy, L.L., E. Burg, C.C. Lenox, L.M. Gauthier, J.M. Petty, M. Antkowiak, T. Palvinskaya, N. Ubags, M. Rincon, A.E. Dixon, et al. 2012. Obesity is associated with neutrophil dysfunction and attenuation of murine acute lung injury. *American Journal of Respiratory Cell and Molecular Biology* 47: 120–127.
11. Meduri, G.U., S. Headley, G. Kohler, F. Stentz, E. Tolley, R. Umberger, and K. Leeper. 1995. Persistent elevation of inflammatory cytokines predicts a poor outcome in ARDS. Plasma IL-1 beta and IL-6 levels are consistent and efficient predictors of outcome over time. *Chest* 107: 1062–1073.
12. Ware, L.B. 2005. Prognostic determinants of acute respiratory distress syndrome in adults: impact on clinical trial design. *Critical Care Medicine* 33: S217–S222.
13. Kim, J.A., and H.S. Park. 2008. White blood cell count and abdominal fat distribution in female obese adolescents. *Metabolism* 57: 1375–1379.
14. Mancuso, P. 2010. Obesity and lung inflammation. *Journal of Applied Physiology (Bethesda, MD: 1985)* 108: 722–728.
15. Miller, L.A., J. Usachenko, R.J. McDonald, and D.M. Hyde. 2000. Trafficking of neutrophils across airway epithelium is dependent upon both thioredoxin- and pertussis toxin-sensitive signaling mechanisms. *Journal of Leukocyte Biology* 68: 201–208.
16. Gungor, N., A.M. Knaapen, A. Munnia, M. Peluso, G.R. Haenen, R.K. Chiu, R.W. Godschalk, and F.J. van Schooten. 2010. Genotoxic effects of neutrophils and hypochlorous acid. *Mutagenesis* 25: 149–154.
17. Wisse, B.E. 2004. The inflammatory syndrome: the role of adipose tissue cytokines in metabolic disorders linked to obesity. *Journal of the American Society of Nephrology* 15: 2792–2800.
18. Fernandez, L.E., and O. Eickelberg. 2012. The impact og TGF-b on lung fibrosis : from targeting to biomarkers. *Proceedings of the American Thoracic Society* 9: 111–116.
19. Walter H. Watson JDR, Jesse Roman: Lung Extracellular matrix and redox regulation. Redox Biology 2015, 8**:**305–315.
20. Nascimento, T.B., F. Baptista Rde, P.C. Pereira, D.H. Campos, A.S. Leopoldo, A.P. Leopoldo, S.A. Oliveira Junior, C.R. Padovani, A.C. Cicogna, and S. Cordellini. 2011. Vascular alterations in high-fat diet-obese rats: role of endothelial L-arginine/NO pathway. *Arquivos Brasileiros de Cardiologia* 97: 40–45.
21. Bradford, M.M. 1976. A rapid and sensitive method for the quantitation of microgram quantities of protein utilizing the principle of protein-dye binding. *Analytical Biochemistry* 72: 248–254.
22. Kliment, C.R., J.M. Englert, L.P. Crum, and T.D. Oury. 2011. A novel method for accurate collagen and biochemical assessment of pulmonary tissue utilizing one animal. *International Journal of Clinical and Experimental Pathology* 4: 349–355.
23. Re, R., N. Pellegrini, A. Proteggente, A. Pannala, M. Yang, and C. Rice-Evans. 1999. Antioxidant activity applying an improved ABTS radical cation decolorization assay. *Free Radical Biology & Medicine* 26: 1231–1237.
24. Aebi, H. 1984. Catalase in vitro. *Methods in Enzymology* 105: 121–126.
25. Flohe, L., and W.A. Gunzler. 1984. Assays of glutathione peroxidase. *Methods in Enzymology* 105: 114–121.
26. Flohe, L., and F. Otting. 1984. Superoxide dismutase assays. *Methods in Enzymology* 105: 93–104.
27. Winterbourn, C.C., and I.H. Buss. 1999. Protein carbonyl measurement by enzyme-linked immunosorbent assay. *Methods in Enzymology* 300: 106–111.

28. Draper, H.H., and M. Hadley. 1990. Malondialdehyde determination as index of lipid peroxidation. *Methods in Enzymology* 186: 421–431.
29. Wang, X., J. Bai, Q. Xue, X.F. Song, C.M. Qiu, X.C. Li, and H.F. Pei. 2016. Tumor necrosis factor-alpha inhibitor protects against myocardial ischemia/reperfusion injury via Notch1 mediated inhibition of oxidative/nitrative stress in traumatic mice. *Zhonghua Xin Xue Guan Bing Za Zhi* 44: 156–160.
30. Jin, C.Q., H.X. Dong, P.P. Cheng, J.W. Zhou, B.Y. Zheng, and F. Liu. 2013. Antioxidant status and oxidative stress in patients with chronic ITP. *Scandinavian Journal of Immunology* 77: 482–487.
31. Wei, M., L. Tu, Y. Liang, J. Liu, Y. Gong, D. Xiao, and Y. Zhang. 2015. The effect of signal transduction pathway of triggering receptor-1 expressed on myeloid cells in acute lung injury induced by paraquat in rats. *Zhonghua Lao Dong Wei Sheng Zhi Ye Bing Za Zhi* 33: 646–651.
32. Suzuki, K., H. Ota, S. Sasagawa, T. Sakatani, and T. Fujikura. 1983. Assay method for myeloperoxidase in human polymorphonuclear leukocytes. *Analytical Biochemistry* 132: 345–352.
33. Hadi, A.M., K.T. Mouchaers, I. Schalij, K. Grunberg, G.A. Meijer, A. Vonk-Noordegraaf, W.J. van der Laarse, and J.A. Belien. 2011. Rapid quantification of myocardial fibrosis: a new macro-based automated analysis. *Cellular Oncology (Dordrecht)* 34: 343–354.
34. Katie Richter, A.K., Taina Pihlajaniemi, Ritva Heljasvaara, and Thomas Kietzmann. 2015. Redox-Fibrosis: Impact of TGFB1 on ROS generators, mediators and functional consequences. *Redox Biology* 6: 344–352.
35. Leone, N., D. Courbon, F. Thomas, K. Bean, B. Jego, B. Leynaert, L. Guize, and M. Zureik. 2009. Lung function impairment and metabolic syndrome: the critical role of abdominal obesity. *American Journal of Respiratory and Critical Care Medicine* 179: 509–516.
36. Wei-Liang Chen, C.-C.W., Wu Li-Wei, Tung-Wei Kao, James Yi-Hsin Chan, Ying-Jen Chen, Ya-Hui Yang, Yaw-Wen Chang, and Tao-Chun Peng. 2014. Relationship between lung function and metabolic syndrome. *PLoS One* 9.
37. McClean, K.M., F. Kee, I.S. Young, and J.S. Elborn. 2008. Obesity and the lung: 1. Epidemiology. *Thorax* 63: 649–654.
38. Itoh, M., T. Suganami, R. Hachiya, and Y. Ogawa. 2011. Adipose tissue remodeling as homeostatic inflammation. *International Journal of Inflammation* 2011: 720926.
39. Itoh, M.S.T., R. Hachiya, and Y. Ogawa. 2011. Adipose tissue remodeling as homeostatic inflammation. *International Journal of Inflammation* 2011: 1–8.
40. Krunkosky, T.M., B.M. Fischer, L.D. Martin, N. Jones, N.J. Akley, and K.B. Adler. 2000. Effects of TNF-alpha on expression of ICAM-1 in human airway epithelial cells in vitro. Signaling pathways controlling surface and gene expression. *American Journal of Respiratory Cell and Molecular Biology* 22: 685–692.
41. American Thoracic Society/European Respiratory Society International Multidisciplinary Consensus Classification of the Idiopathic Interstitial Pneumonias. 2002. This joint statement of the American Thoracic Society (ATS), and the European Respiratory Society (ERS) was adopted by the ATS board of directors, June 2001 and by the ERS Executive Committee, June 2001. *American Journal of Respiratory and Critical Care Medicine* 165: 277–304.
42. Cottam, D.R., P.A. Schaefer, G.W. Shaftan, L. Velcu, and L.D. Angus. 2002. Effect of surgically-induced weight loss on leukocyte indicators of chronic inflammation in morbid obesity. *Obesity Surgery* 12: 335–342.
43. Warnholtz, A., G. Nickenig, E. Schulz, R. Macharzina, J.H. Brasen, M. Skatchkov, T. Heitzer, J.P. Stasch, K.K. Griendling, D.G. Harrison, et al. 1999. Increased NADH-oxidase-mediated superoxide production in the early stages of atherosclerosis: evidence for involvement of the renin-angiotensin system. *Circulation* 99: 2027–2033.
44. Zhang, C., J. Yang, J.D. Jacobs, and L.K. Jennings. 2003. Interaction of myeloperoxidase with vascular NAD(P)H oxidase-derived reactive oxygen species in vasculature: implications for vascular diseases. *American Journal of Physiology. Heart and Circulatory Physiology* 285: H2563–H2572.
45. Wittenberg, J.B., R.W. Noble, B.A. Wittenberg, E. Antonini, M. Brunori, and J. Wyman. 1967. Studies on the equilibria and kinetics of the reactions of peroxidase with ligands. II. The reaction of ferroperoxidase with oxygen. *The Journal of Biological Chemistry* 242: 626–634.
46. Klebanoff, S.J. 2005. Myeloperoxidase: friend and foe. *Journal of Leukocyte Biology* 77: 598–625.
47. Alderton, W.K., C.E. Cooper, and R.G. Knowles. 2001. Nitric oxide synthases: structure, function and inhibition. *The Biochemical Journal* 357: 593–615.
48. Stuehr, D.J., J. Santolini, Z.Q. Wang, C.C. Wei, and S. Adak. 2004. Update on mechanism and catalytic regulation in the NO synthases. *The Journal of Biological Chemistry* 279: 36167–36170.
49. Kubes, P., M. Suzuki, and D.N. Granger. 1991. Nitric oxide: an endogenous modulator of leukocyte adhesion. *Proceedings of the National Academy of Sciences of the United States of America* 88: 4651–4655.
50. Razavi, H.M., F. Wang le, S. Weicker, M. Rohan, C. Law, D.G. McCormack, and S. Mehta. 2004. Pulmonary neutrophil infiltration in murine sepsis: role of inducible nitric oxide synthase. *American Journal of Respiratory and Critical Care Medicine* 170: 227–233.
51. Nevins, W., I.G.L. Todd, and Sergei P. Atamas. 2012. Molecular and cellular mechanism of pulmonary fibrosis. *Fibrogenesis & Tissue Repair* 5: 11.